

The Variational Theory of Complex Rays: a predictive computational tool for complex 3-D mid-frequency acoustic problems

Hervé Riou, Pierre Ladevèze, Louis Kovalevsky

► To cite this version:

Hervé Riou, Pierre Ladevèze, Louis Kovalevsky. The Variational Theory of Complex Rays: a predictive computational tool for complex 3-D mid-frequency acoustic problems. *Acoustics 2012*, Apr 2012, Nantes, France. hal-00811056

HAL Id: hal-00811056

<https://hal.archives-ouvertes.fr/hal-00811056>

Submitted on 23 Apr 2012

HAL is a multi-disciplinary open access archive for the deposit and dissemination of scientific research documents, whether they are published or not. The documents may come from teaching and research institutions in France or abroad, or from public or private research centers.

L'archive ouverte pluridisciplinaire **HAL**, est destinée au dépôt et à la diffusion de documents scientifiques de niveau recherche, publiés ou non, émanant des établissements d'enseignement et de recherche français ou étrangers, des laboratoires publics ou privés.



ACOUSTICS 2012

The Variational Theory of Complex Rays: a predictive computational tool for complex 3-D mid-frequency acoustic problems

H. Riou, P. Ladevèze and L. Kovalevsky

Laboratoire de Mécanique et Technologie, Bât. Léonard de Vinci 61 Av du président Wilson
94235 Cachan Cedex
riou@lmt.ens-cachan.fr

The Variational Theory of Complex Rays (VTCR) is a predictive computational tool that has been developed to solve mid-frequency problems. This is a wave approach that involves exact solutions of the governing equation, and a non classical variational formulation for handling boundary conditions of the problem. No fine discretization is therefore necessary to find an approximated solution, and the model sizes are consequently drastically reduced in comparison with the element based methods. This results in a more efficient prediction technique for vibration problems, especially in the mid-frequency ranges. This presentation discusses how the VTCR can be used for the analysis of complex 3-D acoustic problems. Its performances will be compared to the element-based methods through validation examples, in order to highlight its superior efficiency over the standard numerical prediction techniques.

1 Introduction

In recent years, the use of numerical simulation techniques in design, analysis and optimisation of systems has become an indispensable part of the industrial design process. The standard Galerkin finite element method (FEM [1]) is a well established computer aided engineering tool which is commonly used for the analysis of time-harmonic dynamic problems. However, the use of continuous, piecewise polynomial shape functions leads to very large models and is associated to numerical difficulties, such as the pollution error, which in practice restricts its application to the low-frequency range.

In recent year, a variety of techniques have been proposed to minimise the last cited drawbacks and as a result, increase the practical application range of the FEM to higher frequencies. Among these techniques, we have the predefined reduced bases [2], the Galerkin least-squares FEM [3], the quasi-stabilized finite element method [4], the partition of unity method [5], the generalized finite element method [6], residual-free bubbles [7] and the quasi optimal Petrov-Galerkin method [8]. They have all shown their capacity to reduce computational costs and solve numerical difficulties. However, the range of frequency solved by these methods is still lower than the mid and high-frequency range.

Apart from the FEM and all the last cited methods, there is another family of methods, the so called Trefftz methods [9], which differ from the FEMs by their choice of shape functions. Indeed, instead of using approximated functions, exact solutions of the governing differential equations are used for the expansion of the field variables. These approaches include, for example, a special use of the partition of unity method [10], the ultra-weak variational method [11], the least-squares method [12], the discontinuous enrichment method [13], the element-free Galerkin method [14], the wave boundary element method [15] and the wave-based method [16]. The Variational Theory of Complex Rays (VTCR), developed in this paper, belongs also to the category of the numerical techniques which uses exact solutions of the governing equation to solve the problem. The decisive advantage of such methods (common to all Trefftz methods) is that no refined discretization is necessary, as they use exact solutions of the governing equation. Therefore, the model size and computational effort are considerably reduced compared to element-based methods. The main differences among all these approaches is the treatment of the transmission conditions (between the sub-structures) and the boundary conditions, and the type of shape functions used.

The VTCR was introduced in [17] and is based on an original variational formulation of the problem which was developed in order to allow the approximations within the substructures to be *a priori* independent of one another. Thus,

in each substructure, any type of shape function can be used, as soon as it verifies the governing equation. This gives to the approach a great flexibility and, consequently, efficiency as any type of function with a strong mechanical content can be used without any difficulty. The second feature defining the VTCR is the introduction of two-scale approximations with a strong mechanical content: the solution is described as the superposition of an infinite number of plane waves which satisfy the governing equation exactly. All the wave directions are taken into account. The unknowns of the problem are their amplitudes.

In [18] and [19], the VTCR was used to predict the vibrational response of a 3-D plate assembly. In [20], plates with heterogeneities were taken into account. In [21], this theory was extended to shell structures. The calculation of the vibrational response over a range of frequencies was presented in [22]. The use of the VTCR for transient dynamics problems was covered in [23]. The extension to acoustic problem was made in [24] and its adaptive version was developed in [25]. It was shown through many examples that this approach was capable of finding an accurate solution by using few dofs.

In this paper, the VTCR is extended to three-dimensional (3D) Helmholtz problems. To this effect, the VTCR formulation is first reviewed in Section 2. Then in Section 3, the space of 3-D approximated shape functions that verify the governing equation is defined. Numerical and CPU performance results obtained with the 3-D VTCR are presented in Section 4. Finally, the conclusion of this work and directions for future research are offered in Section 5.

2 The Variational Theory of Complex Rays for Helmholtz problems

2.1 The reference problem

Let us consider a general three dimensional interior steady state dynamic problem on an acoustic cavity Ω , filled with a fluid characterised by its speed of sound c_0 , its density ρ_0 and its damping coefficient η . The steady state dynamic behaviour of Ω is studied at a fixed circular frequency ω . All description quantities can be written thanks to the complex numbers: an amplitude $Q(\mathbf{x})$ is associated to the quantity $Q(\mathbf{x})e^{i\omega t}$, where \mathbf{x} represents the position and $i = \sqrt{-1}$ the imaginary unity.

The problem to be solved is then the following: find the pressure $p \in H^1(\Omega)$ such that:

$$\begin{cases} \Delta p + k^2 p = f & \text{in } \Omega \\ p - Z.L_v(p) = h_d & \text{over } \partial_z \Omega \\ p = p_d & \text{over } \partial_p \Omega \\ L_v(p) = v_d & \text{over } \partial_v \Omega \end{cases} \quad (1)$$

where $k = (1 - i\eta)k_0 = (1 - i\eta)\frac{\omega}{c_0}$ is the wave number, f a loading function, Z an impedance coefficient and $L_v(\square)$ an operator defined as $L_v(\square) = \frac{i}{\rho_0\omega} \frac{\partial \square}{\partial \mathbf{n}} = \frac{i}{\rho_0\omega} \mathbf{n}^T \cdot \nabla(\square)$, \mathbf{n} being the outward normal to $\partial\Omega$. h_d , p_d and v_d denote respectively a prescribed excitation over $\partial_Z\Omega$, a prescribed pressure over $\partial_p\Omega$ and a prescribed velocity over $\partial_v\Omega$.

Let Ω be partitioned into N_Ω non-overlapping sub-cavities Ω_E , and denote $\Gamma_{E,E'} = \partial\Omega_E \cap \partial\Omega_{E'}$. The reference problem (1) becomes: find the pressure $(p_1, \dots, p_E, \dots, p_{N_\Omega}) \in H^1(\Omega_1) \times \dots \times H^1(\Omega_E) \times \dots \times H^1(\Omega_{N_\Omega})$ such that:

$$\left\{ \begin{array}{ll} \Delta p_E + k^2 p_E = f & \text{in } \Omega_E \\ p_E - Z.L_v(p_E) = h_{dE} & \text{over } \partial_Z\Omega_E \\ p_E = p_{dE} & \text{over } \partial_p\Omega_E \\ L_v(p) = v_{dE} & \text{over } \partial_v\Omega_E \\ \left| \begin{array}{l} p_E = p_{E'} \\ L_v(p_E) = -L_v(p_{E'}) \end{array} \right. & \text{over } \Gamma_{E,E'} \end{array} \right. \quad (2)$$

The terms p_E , Z_E , p_{dE} , h_{dE} and v_{dE} correspond to the pressure, the impedance coefficient and the prescribed excitations over the cavity Ω_E , and the last two equations represent the continuity conditions over $\Gamma_{E,E'}$.

2.2 The VTCR formulation

The VTCR formulation is obtained from the boundary value problem (2) by rewriting it in a weak form. The following functional spaces S_{ad}^E and $S_{ad,0}^E$ are required: these spaces of functions satisfying respectively the un-homogeneous and the homogeneous Helmholtz equation (the first equation of problem (1) considering or not the loading function) in the whole sub-cavity Ω_E :

$$S_{ad}^E = \{p_E \in H^1(\Omega_E) \mid \Delta p_E + k^2 p_E = f, \forall \mathbf{x} \in \Omega_E\} \quad (3)$$

$$S_{ad,0}^E = \{p_E \in H^1(\Omega_E) \mid \Delta p_E + k^2 p_E = 0, \forall \mathbf{x} \in \Omega_E\} \quad (4)$$

The VTCR formulation is:

Find $\{(p_1, \dots, p_E, \dots, p_{N_\Omega}) \in S_{ad}^1 \times S_{ad}^E \times \dots \times S_{ad}^{N_\Omega}\}$ such that:

$$\begin{aligned} Re \left\{ \frac{1}{2} \sum_{E=1}^{n_{el}} \int_{\partial_Z\Omega_E} (p_E - Z.L_v(p_E) - h_{dE}) \cdot \overline{L_v(\delta p_E)} dS \right. \\ \left. + \left(\frac{p_E}{Z} - L_v(p_E) - \frac{h_{dE}}{Z} \right) \cdot \delta p_E dS \right. \\ \left. + \sum_{E=1}^{n_{el}} \int_{\partial_p\Omega_E} (p_E - p_{dE}) \cdot \overline{L_v(\delta p_E)} dS \right. \\ \left. + \sum_{E=1}^{n_{el}} \int_{\partial_v\Omega_E} \overline{L_v(p_E) - v_{dE}} \cdot \delta p_E dS \right. \\ \left. + \sum_{E,E' < E} \frac{1}{2} \int_{\Gamma_{E,E'}} ((p_E - p_{E'}) \cdot \overline{L_v(\delta p_E - \delta p_{E'})} \right. \\ \left. + \overline{L_v(p_E + p_{E'})} \cdot (\delta p_E + \delta p_{E'})) dS \right\} = 0 \\ \forall \{(\delta p_1, \delta p_2, \dots, \delta p_{N_\Omega}) \in S_{ad,0}^1 \times S_{ad,0}^E \times \dots \times S_{ad,0}^{N_\Omega}\} \quad (5) \end{aligned}$$

It is shown in [26] that this formulation is equivalent to the reference probleme (2) if there is some damping (through η or the real part of Z).

Then, all that is necessary, in order to develop approximations from the VTCR, is to verify (5) in a finite dimensional subspace $S_{ad}^{E,h}$ of S_{ad}^E (resp. $S_{ad,0}^{E,h}$ and $S_{ad,0}^E$).

2.3 Discretization of the admissible spaces

The solutions of space S_{ad}^E (see (3)) are generated by the sum of a particular solution $p_E^p(\mathbf{x})$ (associated to the loading function f , and computed thanks to the Green functions) and a solution $p_E^0(\mathbf{x})$ that satisfies the homogeneous part of the dynamic equation. For Ω_E of star like form, it is shown in [27] for two dimensional acoustic problems and in [28] for 3D problems that $p_E^0(\mathbf{x})$ belongs to the set of functions generated by an integral distribution of plane waves which satisfy the homogeneous Helmholtz equation, also known as Herglotz wave functions. This distribution of plane waves can be written as

$$p_E^0(\mathbf{x}) = \int_C A_E(C) e^{i\mathbf{k}(C) \cdot (\mathbf{x} - \mathbf{x}_E)} dC \quad (6)$$

where C is the unit circle for 2-D problems and the unit sphere for 3-D problems and \mathbf{x}_E a reference point located in Ω_E . $A_E(C)$ represents the amplitude of the waves over all the direction of propagation in the 2-D or 3-D space, also denoted as the amplitude portrait.

3 The 3-D version of VTCR with spherical harmonics decomposition of plane waves amplitudes

3.1 Pressure field approximation

As presented in section 2.3, the pressure field is sought as a Herglotz wave function. It is an integral repartition of plane waves over all the direction which, for the 3-D case, can be written as:

$$p_E^0(\mathbf{x}) = \int_{\theta=-\pi}^{\pi} \int_{\varphi=0}^{\pi} A_E(\theta, \varphi) \cdot e^{i\mathbf{k}(\theta, \varphi) \cdot (\mathbf{x} - \mathbf{x}_E)} d\theta \sin\theta d\varphi \quad (7)$$

where A_E describes the amplitudes of the plane waves propagating in the (θ, φ) 3-D spherical direction and $\mathbf{k}(\theta, \varphi)$ their wave vectors.

A truncated Laplace serie is used to describe the amplitude portrait $A_E(\theta, \varphi)$. This serie is the 3-D extension of the Fourier serie used in 2-D. Then, apart from the particular solution $p_E^p(\mathbf{x})$ (see section 2.3), the discrete space $S_{ad}^{E,h} \subset S_{ad}^E$ taken in (5) may be written as

$$\begin{aligned} S_{ad}^{E,h} &= span \left\{ \int_{\theta=-\pi}^{\pi} \int_{\varphi=0}^{\pi} Y_l^m(\theta, \varphi) e^{i\mathbf{k}(\theta, \varphi) \cdot (\mathbf{x} - \mathbf{x}_E)} d\theta \sin\theta d\varphi \right. \\ &\quad \left. m = -l, \dots, l, l = 0, \dots, N_E \right\} \\ &= span \left\{ \Phi_l^m(\mathbf{x}), m = -l, \dots, l, l = 0, \dots, N_E \right\} \quad (8) \end{aligned}$$

where $Y_l^m(\theta, \varphi) = \sqrt{\frac{2 \cdot (l-m)!}{(l+m)!}} \cdot P_l^m(\cos\theta) \cdot e^{im\varphi}$, with $P_l^m(X) = \frac{(-1)^m}{2^l \cdot l!} (1-X^2)^{m/2} \frac{\partial^{m+l}(X^2-1)^l}{\partial X^{m+l}}$ the Legendre polynomial, is the spherical harmonics of non negative index l and momentum m . Parameter m varies from $-l$ to l . The set $\{Y_l^m(\theta, \varphi)\}_{|m| \leq l < \infty}$ forms a complete orthogonal system on the unit sphere considering the classic L^2 scalar product.

3.2 Number of shape functions to use

Figure 1 reports the plot of the energy defined by $e_{\Omega_E}(\Phi_l^m) = \frac{1}{\rho_0\omega} \int_{\Omega_E} \Phi_l^m(\mathbf{x}) \overline{\Phi_l^m(\mathbf{x})} d\Omega$ of each shape function Φ_l^m on a 1 m

x 1 m x 1 m cubic cavity Ω filled with air at 1000 Hz. One can see that the energy of the shape functions decreases with order l . Then it is possible to predict the right number of shape function that must be used in 3-D Helmholtz problems to reach a desired precision. Indeed, for a sub-cavity Ω_E , higher index l_{max} must verify:

$$\forall l \leq l_{max} \quad \max_{|m| \leq l} \frac{e_{\Omega_E}(\Phi_l^m)}{e_{\Omega_E}(\Phi_0^0)} \geq 10^{-r} \quad (9)$$

where r is a given number related to the desired precision.

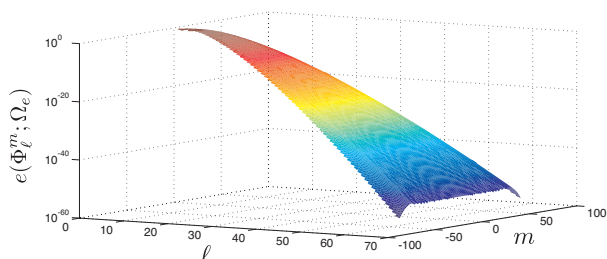


Figure 1: Evolution of the energy of the Fourier VTGR shape functions Φ_l^m versus its order l and momentum m .

4 Numerical results

4.1 Cubic wave guide

First, let us consider a simple cavity. The domain Ω is a cube with dimensions $[0, L] \times [0, L] \times [0, L]$ and the prescribed Robin boundary conditions are $h_d = p_{ex} - Z \cdot L_n(p_{ex})$ such that the exact solution p_{ex} is a plane wave propagating in the spherical direction ($\theta_{ex} = 0.8^\circ, \varphi_{ex} = 2.3^\circ$). This choice has been retained as the wave direction does not correspond to any particular direction in the spherical coordinates. The cavity Ω is taken in its whole geometry, without any discretization in sub-cavities. The convergence with respect to the number of shape functions used in $S_{ad}^{E,h}$ (see (8)) is evaluated for the three considered cases: $kL = 5$, $kL = 10$, and $kL = 15$. The results are visible on Figure 2. The relative

error $\varepsilon(p) = \frac{\|p - p_{ref}\|_{L^2(\Omega)}^2}{\|p_{ref}\|_{L^2(\Omega)}^2}$ of the approximated solutions is used. As one can see, the 3-D VTGR presents a very good convergence rate. Indeed, all the curves rapidly decreases toward very small values. Moreover, even with very small values of r in criterion (9) (for example for $r = 1$ which corresponds to the first point in each decreasing curve) the associated errors are quite small (less than 2% in the present cases).

4.2 Three dimensional car cavity

The 3-D VTGR is used to solve an acoustic problem defined on a car cavity visible on Figure 3. The cavity is filled with air ($\rho_0 = 1,2 \text{ kg.m}^{-3}$, $c_0 = 344 \text{ m.s}^{-1}$ and $\eta = 10^{-5}$) and is excited by a point source located in the front right part of the cavity. As one can see, boundary conditions can be a normal impedance condition with two different impedance values $Z = 845 - 55i \text{ Pa.s.m}^{-1}$ on the seats and $Z = 615.4 - 1887i \text{ Pa.s.m}^{-1}$ on the other boundaries, or a hardwall on the front and rear windows. The decomposition of the cavity in sub-cavities can be seen on Figure 3.

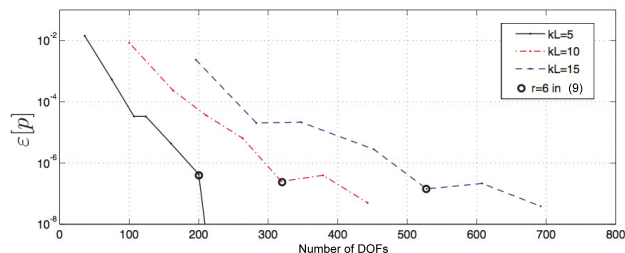


Figure 2: Convergence on the pressure field of the 3-D VTGR for a cubic wave guide problem with dimensions $[0, L] \times [0, L] \times [0, L]$ with Robin boundary conditions (see Section 4.1): $kL = 5$, $kL = 10$ and $kL = 15$.

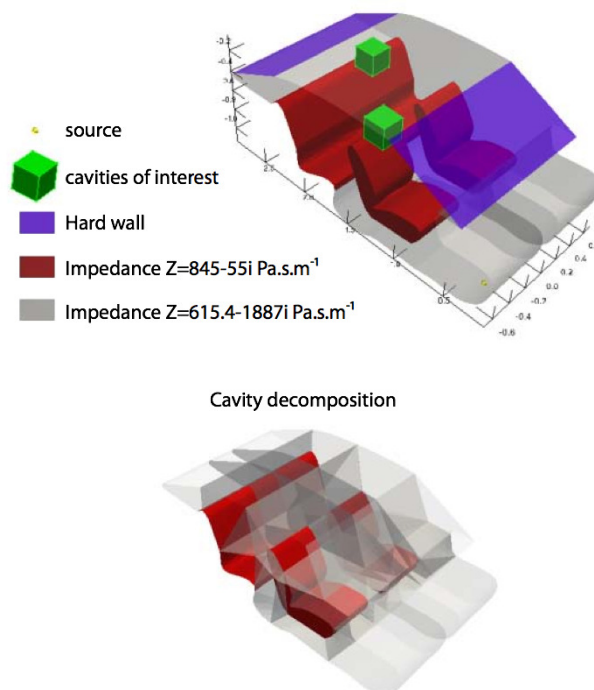


Figure 3: Definition of the car cavity of section 4.2 (boundary conditions and decomposition into sub-cavities).

The solution of this problem at 1700 Hz is plotted on Figure 4. Different spatial snapshots in the car have been represented to show the pressure in the whole cavity. They have been computed for $r = 3$ in criterion (9) leading to 16342 DOFs used.

As the 3-D VTCT permits one to solve such a complex problem, some industrial interesting quantities can be computed. To this effect, we have plotted the RMS average pressure in the two cavities of interest visible on Figure 3. They correspond to the cubic zone of 0.2 m length of the sound "ambiance" near the head of the front and rear passengers. This quantity has been computed on 64 points equally distributed in each cavity of interest. The results can be seen on Figure 5. On that figure, the RMS value has been superposed to the pressure of all the 64 points. Such an information could be interested for the design of the car cavity.

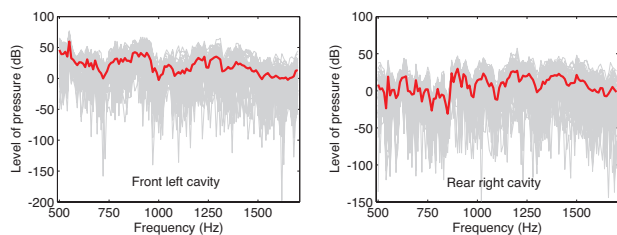


Figure 5: Evolution of the pressure of all the 64 points (grey curves) and the RMS average pressure (red bold line) inside the front left cavity (left) and rear right cavity (right) defined in Figure 3.

5 Conclusion

The extension of the VTCT to 3-D acoustic problems in the medium frequency range is presented. This extension is based on the spherical harmonics expansion of the amplitudes of the plane waves that are used in the VTCT.

Two different examples of different complexities are considered to assess the performances of the 3-D VTCT. The first example shows the excellent convergence rate of the VTCT. The last example, an industrial car cavity, shows that the 3-D VTCT can run on very complex 3-D examples.

Some foregoing future problems are these one: the use of the Fourier approximation in three dimensional assembly of plates; the investigation of vibro-acoustic examples; the definition of a general frameworks for complex structural vibration problems.

Acknowledgments

The authors gratefully acknowledge the ITN Marie Curie project GA-214909 "MID-FREQUENCY - CAE Methodologies for Mid-Frequency Analysis in Vibration and Acoustics".

References

[1] O. C. Zienkiewicz, *The Finite Element Method*, McGraw-Hill, London, 1977.

[2] C. Soize. Reduced models in the medium frequency range for the general dissipative structural dynamic systems. *European Journal of Mechanics and A/Solids*, 17:657-685, 1998.

[3] I. Harari and T.J.R. Hughes. Galerkin/least-squares finite element methods for the reduced wave equation with non- reflecting boundary conditions in unbounded domains, *Computer Methods in Applied Mechanics and Engineering*, 98(3):411-454, 1992.

[4] I. Babuska, F. Ihlenburg, E.T. Paik, and S.A. Sauter. A generalized finite element method for solving the helmholtz equation in two dimensions with minimal pollution. *Computer Methods in Applied Mechanics and Engineering*, 128:325-359, 1995.

[5] J.M. Melenk and I. Babuska. Approximation with harmonic and generalized harmonic polynomials in the partition of unity method. *Computer Assisted Mechanics and Engineering Sciences*, 4:607-632, 1997.

[6] T. Strouboulis, K. Copps, and I. Babuska. The generalized finite element method: an example of its implementation and illustration of its performance, *International Journal for Numerical Methods in Engineering*, 47:1401-1417, 2000.

[7] T.J.R. Hughes. Multiscale phenomena: Greens functions and the dirichlet-to-neumann formulation and subgrid scale models and bubbles and the origins of stabilized methods, *Computer Methods in Applied Mechanics and Engineering*, 127(1-4):387-401, 1995.

[8] A. F. D. Loula and D. T. Fernandes. A quasi optimal Petrov-Galerkin method for Helmholtz problem. *Internat. J. Numer. Methods Engrg.*, 80:1595 - 1622, 2009.

[9] E. Trefftz, Ein gegenstück zum ritzschen verfahren, in: *Second International Congress on Applied Mechanics*, Zürich, Switzerland, 1926.

[10] T. Strouboulis and R. Hidajat, Partition of unity method for helmholtz equation: q-convergence for plane-wave and wave- band local bases, *Applications of Mathematics*, 51(2):181-204, 2006.

[11] O. Cessenat and B. Despres, Application of an ultra weak variational formulation of elliptic pdes to the two-dimensional helmholtz problem, *SIAM Journal on Numerical Analysis*, 35(1):255-299, 1998.

[12] P. Monk and D.Q. Wang, A least-squares method for the helmholtz equation, *Computer Methods in Applied Mechanics and Engineering*, 175:121-136, 1999.

[13] C. Farhat, I. Harari, and L.P. Franca, The discontinuous enrichment method, *Computer Methods in Applied Mechanics and Engineering*, 190:6455-6479, 2001.

[14] P. Bouillard and S. Suleau, Element-free galerkin solutions for helmholtz problems: formulation and numerical assessment of the pollution effect, *Computer Methods in Applied Mechanics and Engineering*, 162(1-4):317-335, 1998.

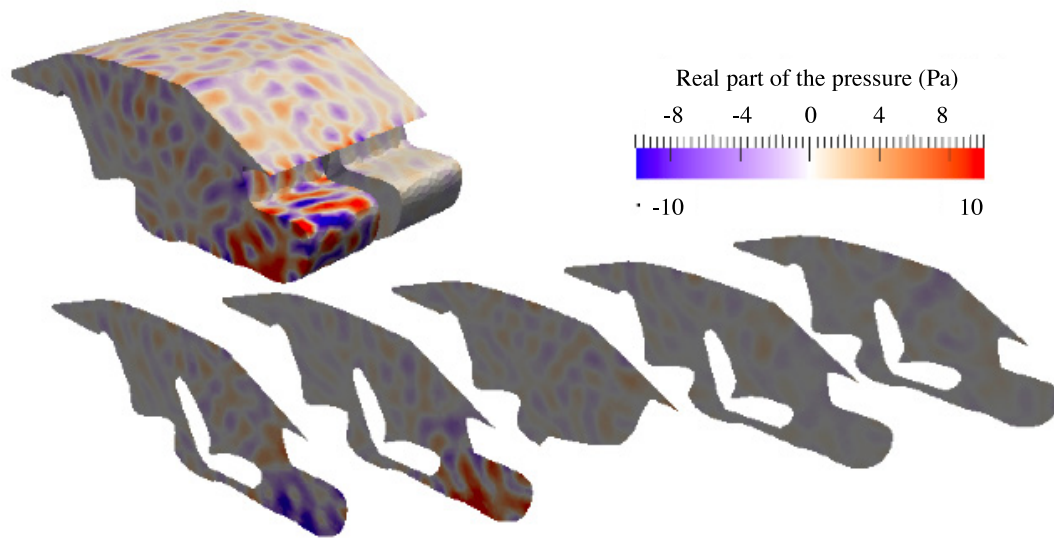


Figure 4: Real part of the pressure field computed with the 3-D VTRC in the problem defined in Figure 3 at 1700 Hz.

- [15] E. Perrey-Debain, J. Trevelyan, and P. Bettess, Wave boundary elements: a theoretical overview presenting applications in scattering of short waves, *Engineering Analysis with Boundary Elements*, 28(2):131-141, 2004.
- [16] W. Desmet, P. Sas and D. Vandepitte, An indirect trefftz method for the steady-state dynamic analysis of coupled vibro-acoustic systems, *Computer Assisted Mechanics and Engineering Sciences*, 8:271-288, 2001.
- [17] P. Ladevèze, A new computational approach for structure vibrations in the medium frequency range, *Comptes Rendus Acadz'mie des Sciences Paris*, 322(IIb):849-856, 1996.
- [18] P. Ladevèze, L. Arnaud, P. Rouch and C. Blanzé, The variational theory of complex rays for the calculation of medium- frequency vibrations, *Engineering Computations*, 18(1-2):193-214, 2001.
- [19] R. Rouch and P. Ladevèze, The variational theory of complex rays: a predictive tool for medium-frequency vibrations, *Computer Methods in Applied Mechanics and Engineering*, 192(28-30):3301-3315, 2003.
- [20] P. Ladevèze, L. Blanc, P. Rouch and C. Blanzé. A multi-scale computational method for medium-frequency vibrations of assemblies of heterogeneous plates, *Computers and Structures*, 81:1267-1276, 2003.
- [21] H. Riou, P. Ladevèze and P. Rouch, Extension of the variational theory of complex rays to shells for medium-frequency vibrations, *Journal of Sound and Vibration*, 272(1-2):341-360, 2004.
- [22] P. Ladevèze, P. Rouch, H. Riou and X. Bohineust, Analysis of medium-frequency vibrations in a frequency range, *Journal of Computational Acoustics*, 11(2):255-284, 2003.
- [23] P. Ladevèze and M. Chevreuil, A new computational method for transient dynamics including the low- and the medium- frequency ranges, *International Journal for Numerical Methods in Engineering*, 64(4):503-527, 2005.
- [24] H. Riou, P. Ladevèze and B. Sourcis, The multiscale VTRC approach applied to acoustics problems, *Journal of Computational Acoustics*, 16(4):487-505, 2008.
- [25] H. Riou, P. Ladevèze, B. Sourcis, B. Faverjon and L. Kovalevsky, An adaptive numerical strategy for the medium-frequency analysis of Helmholtz's problem, *Journal of Computational Acoustics*, accepted.
- [26] L. Kovalevsky, P. Ladevèze, and H. Riou, The Fourier version of the Variational Theory of Complex Rays for medium-frequency acoustics, submitted.
- [27] R. L. Ochs Jr, A version of runge's theorem for the Helmholtz equation with applications to scattering theory, *Proceedings of the Edinburgh Mathematical Society*, 32:107-119, 1989.
- [28] D. Colton and R. Kress, On the denseness of Herglotz wave functions and electromagnetic Herglotz pairs in Sobolev spaces, *Mathematical methods in the applied sciences*, 24:1289-1303, 2001.